Acta Crystallographica Section B
Structural Science
ISSN 0108-7681

Isomeric iodo-*N*-(nitrobenzyl)anilines: interplay of hard and soft hydrogen bonds, iodo···nitro interactions and aromatic $\pi\cdots\pi$ stacking interactions

Christopher Glidewell,[a]* John N. Low,[b]‡ Janet M. S. Skakle,[b] Solange M. S. V. Wardell[c]§ and James L. Wardell[d]

[a]School of Chemistry, University of St Andrews, St Andrews, Fife KY16 9ST, Scotland, [b]Department of Chemistry, University of Aberdeen, Meston Walk, Old Aberdeen AB24 3UE, Scotland, [c]Instituto de Química, Departamento de Química Orgânica, Universidade Federal Fluminense, 24020-150 Niterói, Rio de Janeiro-RJ, Brazil, and [d]Instituto de Química, Departamento de Química Inorgânica, Universidade Federal do Rio de Janeiro, CP 68563, 21945-970 Rio de Janeiro-RJ, Brazil

‡ Postal address: School of Engineering and Physics, University of Dundee, Dundee DD1 4HN, Scotland
§ Present address: Fundação Oswaldo Cruz, Far Manguinhos, Rua Sizenando Nabuco, 100 Manguinhos, 21041250 Rio de Janeiro, RJ Brazil.

Correspondence e-mail: cg@st-andrews.ac.uk

Received 28 April 2004
Accepted 17 May 2004

Molecules of 2-iodo-*N*-(4-nitrobenzyl)aniline, 4-$O_2NC_6H_4CH_2NHC_6H_4I$-2′ (1) are linked into chains by C—H···O hydrogen bonds. In the isomeric compound 3-iodo-*N*-(4-nitrobenzyl)aniline (2) a combination of N—H···O and C—H···O hydrogen bonds and iodo···nitro and aromatic $\pi\cdots\pi$ stacking interactions links the molecules into a three-dimensional framework structure. The two-dimensional supramolecular structure of 4-iodo-*N*-(4-nitrobenzyl)aniline (6) is built from a combination of C—H···O and N—H···π(arene) hydrogen bonds and aromatic $\pi\cdots\pi$ stacking interactions. 2-Iodo-*N*-(2-nitrobenzyl)aniline (7) crystallizes with two molecules in the asymmetric unit and these molecules are linked into ladders by a combination of N—H···O and C—H···O hydrogen bonds and iodo···nitro and aromatic $\pi\cdots\pi$ stacking interactions. Comparisons are made between the supramolecular structures of these compounds and those of other isomers, in terms both of the types of direction-specific intermolecular interactions exhibited and the dimensionality of the resulting supramolecular structures.

1. Introduction

As part of a general study of the interplay of hydrogen bonds, iodo···nitro interactions and aromatic $\pi\cdots\pi$ stacking interactions in aromatic systems containing both iodo and nitro substituents, we have recently reported the molecular and supramolecular structures of a range of diaryl species [see (I)] containing a variety of *X* spacer units, including arenesulfonamides (*A*) and (*B*) (Kelly *et al.*, 2002) and Schiff-base imines (*C*) (Wardell *et al.*, 2002) and (*D*) (Glidewell, Howie *et al.*, 2002), together with some benzylanilines (*E*) (Glidewell, Low *et al.*, 2002).

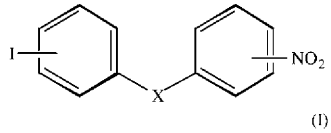

(I)

(A) X = -SO_2-NH-
(B) X = -NH-SO_2-
(C) X = -CH=N-
(D) X = -N=CH-
(E) X = -NH-CH_2-

In the case of the Schiff-base imines of type (*D*), we were able to study the supramolecular aggregation modes in eight of the possible nine isomers (Glidewell, Howie *et al.*, 2002), although the structure of the 4,4′-isomer, which crystallizes with $Z' = 2$ in space group *Fdd*2, proved to be elusive because of the intractable disorder. In this series the interplay of the various weak intermolecular interactions is such that neither the supramolecular structure nor even the range of interactions involved can readily be predicted for any single example from a detailed knowledge of all the rest of the series. With

this in mind, we have now expanded our preliminary study (Glidewell, Low *et al.*, 2002) of the benzylanilines (*E*) to incorporate a total of six isomers of this series, (1), (2) and (4)–(7) [see (II)].

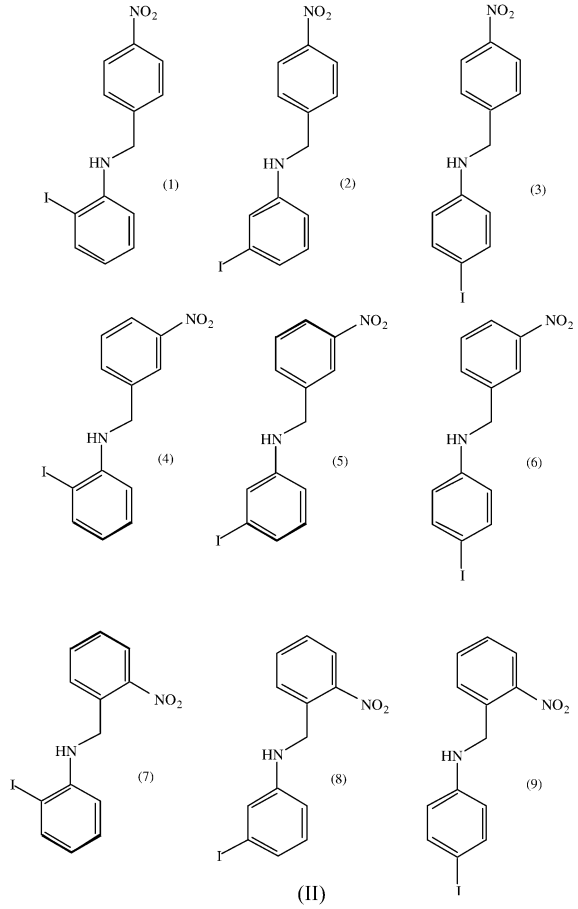

(II)

2. Experimental

2.1. Synthesis

Nitrobenzylidene-iodoanilines were prepared as previously described (Glidewell, Howie *et al.*, 2002) and subsequently reduced using a fivefold molar excess of sodium borohydride in refluxing methanol. After work-up, crystals of (1), (2), (6) and (7) suitable for single-crystal X-ray diffraction were grown by slow evaporation of solutions in ethanol. Compound (8) is an oil at ambient temperature and we have not been able to induce crystallization, even at reduced temperatures: (3) and (4) are solids at ambient temperature but, despite repeated efforts, we have so far been unable to obtain any crystals of either compound which are suitable for single-crystal X-ray diffraction.

2.2. Data collection, structure solution and refinement

Diffraction data for (1), (2), (6) and (7) were collected at 120 (2) K using a Nonius Kappa-CCD diffractometer with graphite-monochromated Mo $K\alpha$ radiation (λ = 0.71073 Å).

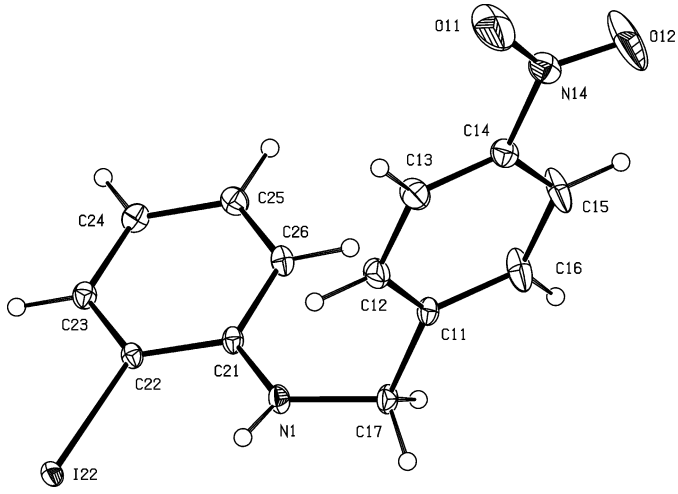

Figure 1
A molecule of (1), showing the atom-labelling scheme. Displacement ellipsoids are drawn at the 30% probability level.

Other details of the cell data, data collection and refinement are summarized in Table 1, together with details of the software employed (Ferguson, 1999; Nonius, 1997; Otwinowski & Minor, 1997; Sheldrick, 1997*a*,*b*; McArdle, 2003).[1]

For (1) and (6) the space group $P2_1/c$ was uniquely assigned from the systematic absences: likewise, the space group $P2_12_12_1$ was uniquely assigned for (2). Compound (7) is triclinic, and the space group $P\bar{1}$ was selected and confirmed by the subsequent analysis. The structures were solved by direct methods and refined with all data on F^2. A weighting scheme based upon $P = [F_o^2 + 2F_c^2]/3$ was employed in order to reduce statistical bias (Wilson, 1976). All H atoms were located from difference maps and they were included in the refinements as riding atoms with the bond distances C—H 0.95 (aromatic) or 0.99 Å (CH_2) and N—H 0.88 Å. The absolute configuration of (2) in the crystal selected for study was established by the use of the Flack parameter (Flack, 1983), whose final value was −0.01 (2) with 1191 Friedel pairs present.

Supramolecular analyses were made and the diagrams were prepared with the aid of *PLATON* (Spek, 2003). Details of molecular conformations are given in Table 2. Details of hydrogen-bond dimensions and short intramolecular contacts, and iodo···nitro interactions are given in Tables 3 and 4. Figs. 1–13 show the molecular components, with the atom-labelling schemes, and aspects of the supramolecular structures.

3. Results and discussion

3.1. Molecular conformations

The molecular conformations of iodo-(*N*-benzyl)anilines can be defined in terms of just four torsional angles and these are given in Table 2 for (1), (2) and (4)–(7). For the central

[1] Supplementary data for this paper are available from the IUCr electronic archives (Reference: NA5018). Services for accessing these data are described at the back of the journal.

Table 1
Experimental details.

	(1)	(2)	(6)	(7)
Crystal data				
Chemical formula	$C_{13}H_{11}IN_2O_2$	$C_{13}H_{11}IN_2O_2$	$C_{13}H_{11}IN_2O_2$	$C_{13}H_{11}IN_2O_2$
M_r	354.14	354.14	354.14	354.14
Cell setting, space group	Monoclinic, $P2_1/c$	Orthorhombic, $P2_12_12_1$	Monoclinic, $P2_1/c$	Triclinic, $P\bar{1}$
a, b, c (Å)	16.1564 (6), 9.3589 (3), 8.3326 (3)	7.0966 (2), 12.5908 (4), 13.8360 (6)	21.2778 (15), 8.1809 (5), 7.2793 (4)	8.16850 (10), 10.8834 (2), 15.4372 (2)
α, β, γ (°)	90.00, 96.3330 (10), 90.00	90.00, 90.00, 90.00	90.00, 94.316 (2), 90.00	76.9219 (9), 80.0727 (7), 74.2167 (7)
V (Å^3)	1252.25 (8)	1236.27 (8)	1263.53 (14)	1277.36 (3)
Z	4	4	4	4
D_x (Mg m^{-3})	1.878	1.903	1.862	1.841
Radiation type	Mo $K\alpha$	Mo $K\alpha$	Mo $K\alpha$	Mo $K\alpha$
No. of reflections for cell parameters	2850	2783	2785	5760
θ range (°)	3.3–27.5	2.9–27.5	3.1–27.5	3.1–27.5
μ (mm^{-1})	2.55	2.59	2.53	2.50
Temperature (K)	120 (2)	120 (2)	120 (2)	120 (2)
Crystal form, colour	Block, red	Needle, orange	Needle, yellow	Block, orange
Crystal size (mm)	0.32 × 0.22 × 0.15	0.38 × 0.05 × 0.03	0.48 × 0.04 × 0.02	0.22 × 0.18 × 0.12
Data collection				
Diffractometer	Kappa-CCD	Kappa-CCD	Kappa-CCD	Kappa-CCD
Data collection method	φ scans, and ω scans with κ offsets	φ scans, and ω scans with κ offsets	φ scans, and ω scans with κ offsets	φ scans, and ω scans with κ offsets
Absorption correction	Multi-scan	Multi-scan	Multi-scan	Multi-scan
T_{min}	0.496	0.440	0.377	0.597
T_{max}	0.682	0.927	0.951	0.738
No. of measured, independent and observed reflections	8013, 2850, 2641	9541, 2783, 2437	12 705, 2785, 1934	5760, 5760, 5317
Criterion for observed reflections	$I > 2\sigma(I)$	$I > 2\sigma(I)$	$I > 2\sigma(I)$	$I > 2\sigma(I)$
R_{int}	0.050	0.050	0.064	0.046
θ_{max} (°)	27.5	27.5	27.5	27.5
Range of h, k, l	$-20 \Rightarrow h \Rightarrow 20$ $-11 \Rightarrow k \Rightarrow 12$ $-7 \Rightarrow l \Rightarrow 10$	$-8 \Rightarrow h \Rightarrow 9$ $-16 \Rightarrow k \Rightarrow 16$ $-15 \Rightarrow l \Rightarrow 17$	$-27 \Rightarrow h \Rightarrow 27$ $-10 \Rightarrow k \Rightarrow 10$ $-9 \Rightarrow l \Rightarrow 9$	$-10 \Rightarrow h \Rightarrow 10$ $-14 \Rightarrow k \Rightarrow 13$ $-20 \Rightarrow l \Rightarrow 20$
Refinement				
Refinement on	F^2	F^2	F^2	F^2
$R[F^2 > 2\sigma(F^2)]$, $wR(F^2)$, S	0.028, 0.067, 1.08	0.030, 0.050, 1.01	0.035, 0.065, 1.00	0.038, 0.106, 1.14
No. of reflections	2850	2783	2785	5760
No. of parameters	163	163	163	325
H-atom treatment	Constrained to parent site	Constrained to parent site	Constrained to parent site	Constrained to parent site
Weighting scheme	$= 1/[\sigma^2(F_o^2) + (0.0212P)^2 + 2.0006P]$, where $P = (F_o^2 + 2F_c^2)/3$	$w = 1/[\sigma^2(F_o^2) + (0.0137P)^2]$, where $P = (F_o^2 + 2F_c^2)/3$	$w = 1/[\sigma^2(F_o^2) + (0.0209P)^2]$, where $P = (F_o^2 + 2F_2^c)/3$	$w = 1/[\sigma^2(F_o^2) + (0.0523P)^2 + 2.2937P]$, where $P = (F_o^2 + 2F_c^2)/3$
$(\Delta/\sigma)_{max}$	0.001	0.001	0.001	0.003
$\Delta\rho_{max}$, $\Delta\rho_{min}$ (e Å^{-3})	1.10, −0.74	0.54, −0.61	1.13, −0.60	0.71, −1.65
Absolute structure	–	Flack (1983), 1191 Friedel pairs	–	–
Flack parameter	–	−0.01 (2)	–	–

Computer programs used : *Kappa-CCD server software* (Nonius, 1997), *DENZO-SMN* (Otwinowski & Minor, 1997), *SHELXS*97 (Sheldrick, 1997*b*), *OSCAIL* (McArdle, 2003), *SHELXL*97 (Sheldrick, 1997*a*), *PLATON* (Spek, 2003), *PRPKAPPA* (Ferguson, 1999).

spacer unit, the torsional angle C11—C17—N1—C21 shows that for (2) this unit is essentially *trans* planar, whereas for all other examples discussed here this torsional angle is close to ±90°, indicative of a markedly non-planar unit. The iodinated ring C21–C26 is generally nearly co-planar with the fragment C21—N1—C17. Since the labelling of the iodinated ring is determined by the location of the I substituent, the values show, for example, that in (1) and (2) the I substituent lies off different edges of the molecule: thus in (1) the I is on the same edge as the N—H bond, while in (2) it is on the opposite edge (Figs. 1 and 3). It seems possible that the short intramolecular N—H···I contacts in (1) (Table 3) play a significant role in controlling the overall conformation of (I). Likewise in the 2-iodo derivative (7), there is a short intramolecular N—H···I contact which may be significant in controlling the orientation of the iodinated ring. A similar difference occurs between (4) and (5) (Glidewell, Low *et al.*, 2002). In (2) and (7), as well as in (4), the nitrated ring is nearly co-planar with the adjacent C11—C17—N1 fragment, but this is far from the case in (1), (5) and (6). In all cases there are some fairly short intramo-

Table 2
Selected torsional angles (°).

C11—C17—N1—C21	C12—C11—C17—N1	C17—N1—C21—C22	C—C—N—O11
(1)			
79.3 (3)	37.1 (4)	165.7 (2)	−9.2 (5)[i]
(2)			
−176.0 (3)	−175.9 (3)	17.7 (6)	4.2 (5)[i]
(4)†			
−84.4 (3)	−167.5 (2)	162.8 (2)	−0.9 (3)[ii]
(5)†			
63.7 (3)	45.5 (3)	18.2 (3)	−169.3 (2)[ii]
(6)			
87.8 (4)	43.3 (4)	−16.5 (5)	−5.8 (5)[ii]
(7) Molecule 1‡			
86.5 (4)	174.7 (3)	175.2 (3)	14.5 (5)[iii]
(7) molecule 2‡			
−81.6 (4)	166.4 (3)	−168.2 (3)	36.5 (4)[iv]

(i) C13—C14—N14—O11; (ii) C12—C13—N13—O11; (iii) C11—C12—N12—O11; (iv) C31—C32—N32—O31 † Atoms labelled as for (1), (2), (6) and (7): for the original labelling scheme see Glidewell, Low *et al.* (2002). ‡ For the atom labels in the two independent molecules, see Fig. 11.

Table 3
Parameters (Å, °) for hydrogen bonds and short intramolecular contacts.

D—H···*A*	H···*A*	*D*···*A*	*D*—H···*A*	Motif	Direction
(1)					
C13—H13···O11[i]	2.47	3.403 (5)	167	$R_2^2(10)$	–
C26—H26···O12[ii]	2.55	3.272 (4)	132	$R_2^2(22)$	–
N1—H1···I22	2.77	3.238 (2)	114	*S*(5)	–
C13—H13···O11	2.46	2.731 (4)	96	*S*(5)	–
C15—H15···O12	2.46	2.729 (5)	96	*S*(5)	–
(2)					
N1—H1···O11[iii]	2.53	3.195 (4)	133	*C*(9)	[010]
C17—H172···O11[iv]	2.43	3.357 (5)	156	*C*(8)	[001]
C13—H13···O11	2.44	2.718 (5)	97	*S*(5)	-
C15—H15···O12	2.43	2.721 (5)	98	*S*(5)	–
(6)					
C16—H16···O11[v]	2.48	3.416 (5)	170	*C*(7)	[010]
N1—H1···Cg2[vi]†	2.87	3.563 (4)	137	–	[001]
C12—H12···O11	2.40	2.704 (5)	98	*S*(5)	–
C14—H14···O12	2.45	2.737 (5)	97	*S*(5)	–
(7)					
N3—H3···O12	2.34	3.107 (4)	146	*D*	–
C33—H33···O11[vii]	2.53	3.147 (5)	123	$R_4^4(20)$	–
N1—H1···I22	2.73	3.234 (3)	118	*S*(5)	–
C13—H13···O12	2.36	2.672 (5)	99	*S*(5)	–
C17—H171···O11	2.43	2.688 (5)	94	*S*(6)	–
C17—H172···O11	2.47	2.688 (5)	92	*S*(6)	–
N3—H3···I42	2.75	3.231 (3)	116	*S*(5)	–
C33—H33···O32	2.51	2.758 (4)	95	*S*(5)	–
C37—H371···O31	2.52	2.753 (4)	93	*S*(6)	–
C37—H372···O31	2.49	2.753 (4)	95	*S*(6)	–

Symmetry codes: (i) $-x, 1-y, 1-z$; (ii) $-x, 2-y, 1-z$; (iii) $1-x, \frac{1}{2}+y, \frac{3}{2}-z$; (iv) $\frac{1}{2}-x, -y, -\frac{1}{2}+z$; (v) $x, -1+y, z$; (vi) $x, \frac{3}{2}-y, -\frac{1}{2}+z$; (vii) $1-x, -y, 1-z$. † Cg2 is the centroid of the ring C21–C26.

lecular C—H···O contacts (Table 3). The biggest deviation of the nitro group from co-planarity with the adjacent aryl ring occurs in (7), where moreover the two molecules show a marked difference: apart from this, the molecules in the selected asymmetric unit are close to being mirror images (see Fig. 11). It will be noted (see §3.2) that the structures of all these compounds exhibit direction-specific intermolecular interactions and it is thus probable that the energies associated with these intermolecular interactions are of similar magnitudes to the potential-energy barriers associated with rotation about the single bonds specified in Table 2.

One consequence of the conformational behaviour revealed by the torsional angles is that each molecule is chiral in the solid state, having no internal symmetry whatsoever. Compounds (1), (6) and (7) all crystallize in centrosymmetric space groups containing equal numbers of the two enantiomeric forms, as do (4) and (5) [$P2_1/n$ and *Pbca*, respectively (Glidewell, Low *et al.*, 2002)]: however, (2) crystallizes in the chiral space group $P2_12_12_1$ where each crystal can contain only one enantiomer. Since (2) is almost certainly racemic in solution, its crystallization is as a conglomerate: while the absolute configuration of the molecules in the crystal selected for study was readily determined, this configuration has no chemical significance.

The bond lengths and inter-bond angles show no unusual values.

3.2. Supramolecular structures

3.2.1. Compound (1). In (1) (Fig. 1) there are neither N—H···O or *X*—H···π(arene) hydrogen bonds (where *X* = C or N) nor iodo···nitro or aromatic π···π stacking interactions. The only direction-specific interactions between the molecules are two independent C—H···O hydrogen bonds (Table 2), which combine to link the molecules into chains.

Atom C13 in the nitrated ring of the molecule at (x, y, z) acts as a hydrogen-bond donor to nitro O11 in the molecule at $(-x, 1-y, 1-z)$, so generating by inversion an $R_2^2(10)$ ring centred at $(0, \frac{1}{2}, \frac{1}{2})$: atom C26 in the iodinated ring at (x, y, z) similarly acts as a hydrogen-bond donor to O12 at $(-x, 2-y, 1-z)$, producing an $R_2^2(22)$ ring centred at $(0, 1, \frac{1}{2})$. The propagation by inversion of these two motifs thus generates a chain of rings running parallel to the [010] direction (Fig. 2).

3.2.2. Compound (2). The supramolecular structure of (2) (Fig. 3), in contrast to that of (1), contains both N—H···O and C—H···O hydrogen bonds (Table 2) as well as both iodo···nitro interactions (Table 3) and aromatic π···π stacking interactions: as a result, this structure is three-

Table 4
Parameters for iodo···nitro interactions (Å, °).

C—I···O—N	I···O	C—I···O	I···O—N	Motif[a]	Direction
(2)					
C23—I23···O12^{i}—N14^{i}	3.249 (3)	163.2 (2)	161.6 (2)	*C*(12)	[001]
(4)†					
C2—I2···O131^{i}—N13^{i}	3.517 (2)	158.12 (7)	101.4 (2)	*C*(10)	[001]
(7)					
C42—I42···O32^{ii}—N32^{ii}	3.523 (3)	103.3 (2)	117.1 (2)	*C*(9)	[1$\bar{1}$0]

Reference: (*a*) Starbuck *et al.* (1999). Symmetry codes: (i) $x, y, -1+z$; (ii) $-1+x, 1+y, z$. † Original atom-labelling (Glidewell, Low *et al.*, 2002).

dimensional, as opposed to the one-dimensional aggregation in (1). It is convenient to analyse the formation of the three-dimensional supramolecular network in (2) in terms of chains running parallel to the [100], [010] and [001] directions. There is an N—H···O hydrogen bond, albeit rather weak, which generates a *C*(9) chain running parallel to the [010] direction: N1 in the molecule at (x, y, z) acts as a hydrogen-bond donor to O11 in the molecule at $(1-x, \frac{1}{2}+y, \frac{3}{2}-z)$, thereby producing a chain generated by the 2_1 screw axis along $(\frac{1}{2}, y, \frac{3}{4})$ (Fig. 4).

The [001] chain formation involves both the iodo···nitro interaction and the C—H···O hydrogen bond. The C17 atom at (x, y, z) acts as a hydrogen-bond donor, *via* H172, to O11 at $(\frac{1}{2}-x, -y, -\frac{1}{2}+z)$, so producing a *C*(8) chain generated by the 2_1 screw axis along $(\frac{1}{4}, 0, z)$. At the same time, there is a fairly short two-centre iodo···nitro interaction between I23 in the molecule at (x, y, z) and O12 in that at $(x, y, -1+z)$, which generates by translation a *C*(12) chain along [001]. The combination of the two [001] motifs generates a chain of edge-fused $R_3^3(18)$ rings (Fig. 5).

These two chain types, parallel to [010] and [001], combine to form sheets parallel to (100) and these are linked by a combination of the two types of hydrogen bond. Atom N1 in the molecule at $(\frac{1}{2}+x, \frac{1}{2}-y, 1-z)$, which lies in the (100) sheet in the domain $0.07 < x < 0.93$, acts as a hydrogen-bond donor to O11 in the molecule at $(\frac{3}{2}-x, -y, -\frac{1}{2}+z)$, which forms part of the (100) sheet in the domain $1.07 < x < 1.93$, and the resulting [100] chain (Fig. 6) links all of the (100) sheets into a three-dimensional framework. This linking of the (100) sheets is reinforced by $\pi\cdots\pi$ stacking interactions. The

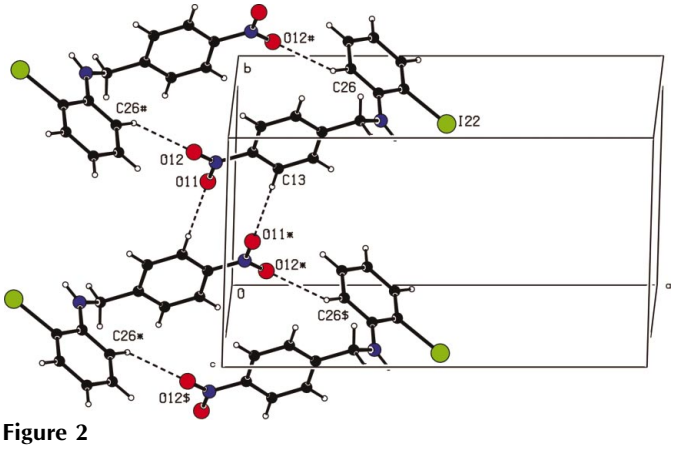

Figure 2
Part of the crystal structure of (1) showing the formation of a chain of $R_2^2(10)$ and $R_2^2(22)$ rings along [010]. The atoms marked with an asterisk (*), a hash (#) or a dollar sign ($) are at the symmetry positions $(-x, 1-y, 1-z)$, $(-x, 2-y, 1-z)$ and $(x, -1+y, z)$, respectively.

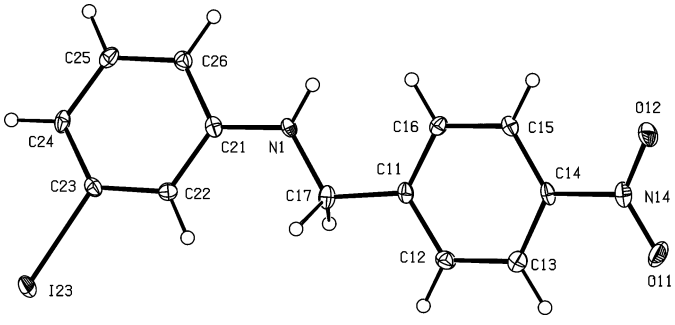

Figure 3
A molecule of (2), showing the atom-labelling scheme. Displacement ellipsoids are drawn at the 30% probability level.

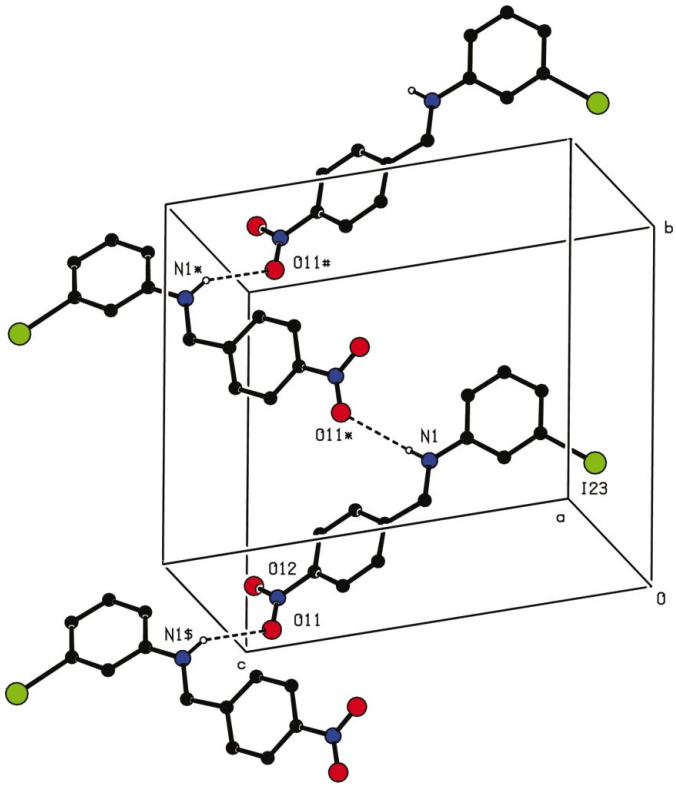

Figure 4
Part of the crystal structure of (2) showing the formation of a *C*(9) chain along [010]. For the sake of clarity, H atoms bonded to C atoms are omitted. The atoms marked with an asterisk (*), a hash (#) or a dollar sign ($) are at the symmetry positions $(1-x, \frac{1}{2}+y, \frac{3}{2}-z)$, $(x, 1+y, z)$ and $(1-x, -\frac{1}{2}+y, \frac{3}{2}-z)$, respectively.

nitrated ring in the molecule at (x, y, z) makes an angle of only 4.1° with the iodinated rings of the two molecules at $(-\frac{1}{2}+x, \frac{1}{2}-y, 1-z)$ and $(\frac{1}{2}+x, \frac{1}{2}-y, 1-z)$: the interplanar spacings are both *ca* 3.45 Å with ring-centroid separations of 3.674 (5) and 3.760 (5) Å, respectively (Fig. 7).

3.2.3. Compound (6). The supramolecular aggregation in (6) (Fig. 8) exhibits neither N—H···O hydrogen bonds nor iodo···nitro interactions: instead, the C—H···O hydrogen bond and the aromatic $\pi\cdots\pi$ stacking interaction are augmented by an N—H···π(arene) hydrogen bond, which forms in preference to the N—H···O hydrogen bond which might have been expected here. A single C—H···O hydrogen bond which involves a nitro O atom as an acceptor generates a simple chain running parallel to the [010] direction. Atom C16 in the nitrated ring of the molecule at (x, y, z) acts as a hydrogen-bond donor to O11 in the molecule at $(x, 1+y, z)$, so generating by translation a $C(7)$ chain along [010] (Fig. 9).

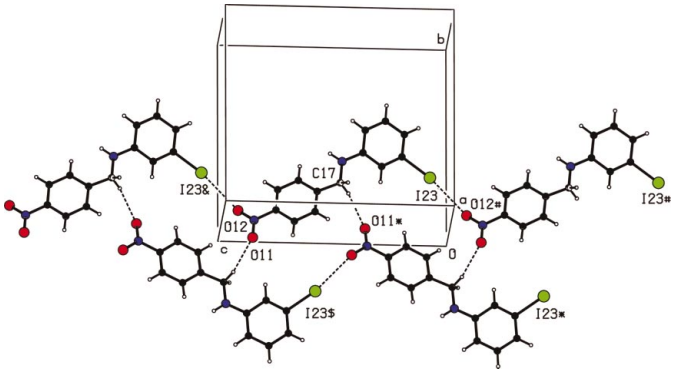

Figure 5
Part of the crystal structure of (2) showing the formation of a [001] chain built from C—H···O hydrogen bonds and iodo···nitro interactions. The atoms marked with an asterisk (*), a hash (#), a dollar sign ($) or an ampersand (&) are at the symmetry positions $(\frac{1}{2}-x, -y, -\frac{1}{2}+z)$, $(x, y, -1+z)$, $(\frac{1}{2}-x, -y, \frac{1}{2}+z)$ and $(x, y, 1+z)$, respectively.

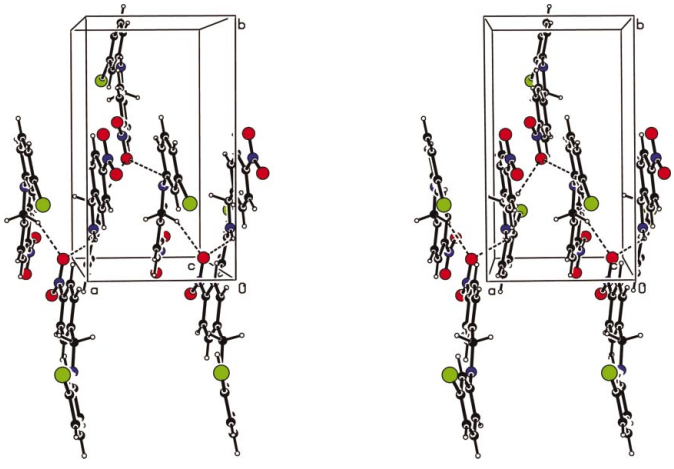

Figure 6
Stereoview of part of the crystal structure of (2) showing the formation of a [100] chain built from N—H···O and C—H···O hydrogen bonds.

The N—H···π(arene) hydrogen bond combines with the $\pi\cdots\pi$ stacking interactions to generate chains running parallel to the [001] direction. Amino atom N1 in the molecule at (x, y, z) acts as a hydrogen-bond donor to the iodinated ring C21–C26, centroid Cg2 (Table 2), of the molecule at $(x, \frac{3}{2}-y, -\frac{1}{2}+z)$. At the same time, the nitrated ring of the molecule at (x, y, z) forms $\pi\cdots\pi$ stacking interactions with the corresponding rings of the molecules at $(x, \frac{3}{2}-y, \frac{1}{2}+z)$ and $(x, \frac{3}{2}-y, -\frac{1}{2}+z)$: the angle between the adjacent rings is only *ca* 1.6°, and the centroid separation and the interplanar spacing are 3.844 (5) and *ca* 3.45 Å, respectively, corresponding to a centroid offset of *ca* 1.74 Å. Propagation of the mutually cooperative and mutually reinforcing N—H···π and $\pi\cdots\pi$ interactions thus produces a chain along [001] generated by the *c*-glide plane at $y = 0.75$ (Fig. 10). The combination of [010] and [001] chains generates a sheet parallel to (100), but there are no direction-specific interactions between adjacent sheets.

3.2.4. Compound (7). Compound (7) (Fig. 11) crystallizes with $Z' = 2$ in space group $P\bar{1}$: within the selected asymmetric unit, N3 in molecule 2 (containing N3 and I42) acts as a

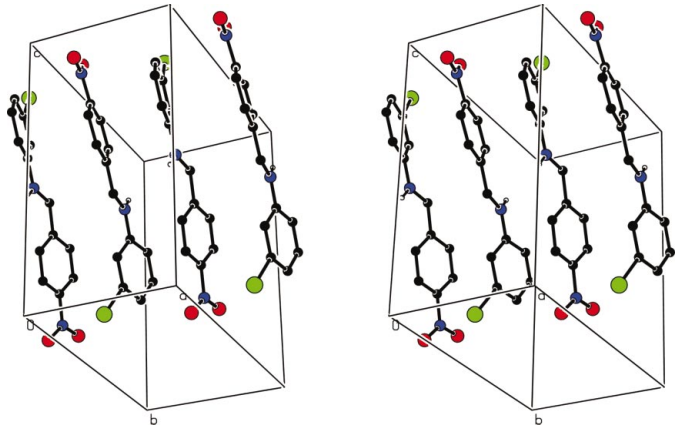

Figure 7
Stereoview of part of the crystal structure of (2) showing the aromatic $\pi\cdots\pi$ stacking along [100]. For the sake of clarity, H atoms bonded to C atoms are omitted.

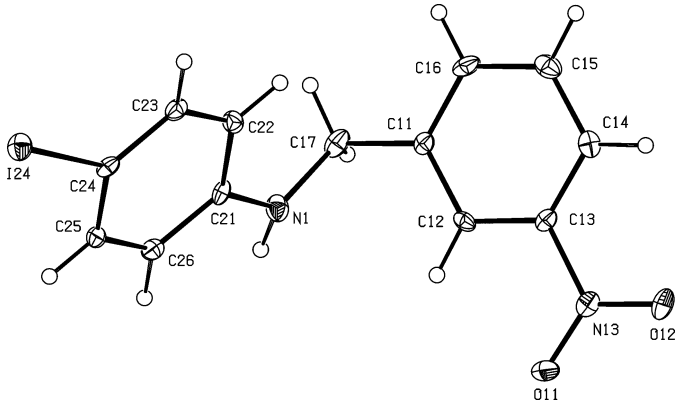

Figure 8
A molecule of (6), showing the atom-labelling scheme. Displacement ellipsoids are drawn at the 30% probability level.

hydrogen-bond donor to O12 in molecule 1 (containing N1 and I22), but N1 does not participate in any intermolecular hydrogen bonding. This difference in behaviour between N1 and N3 suffices to preclude any possibility of additional symmetry. In addition to the single N—H···O hydrogen bond within the asymmetric unit, the molecules are further linked into molecular ladders by a single, rather weak C—H···O hydrogen bond and a single, rather weak iodo···nitro interaction, whose action is reinforced by two independent aromatic $\pi\cdots\pi$ stacking interactions.

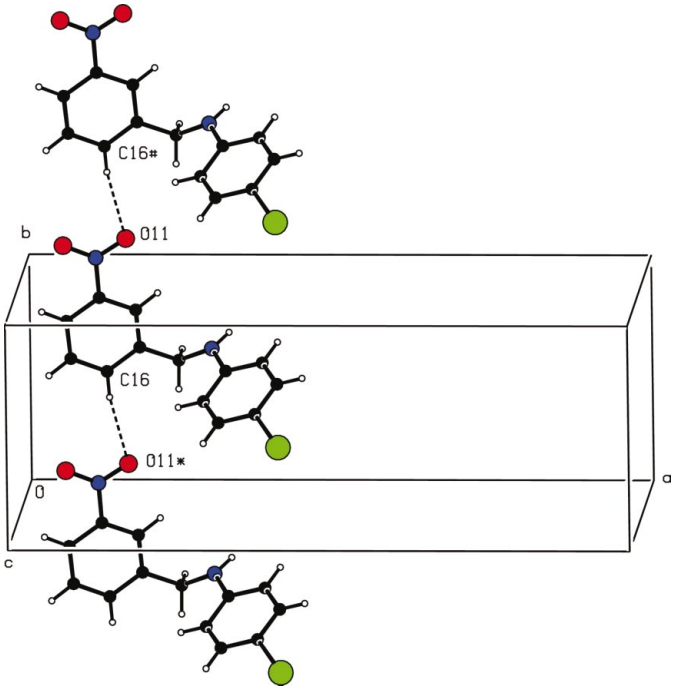

Figure 9
Part of the crystal structure of (6) showing the formation of a $C(7)$ chain along [010]. The atoms marked with an asterisk (*) or a hash (#) are at the symmetry positions $(x, 1 + y, z)$ and $(x, -1 + y, z)$, respectively.

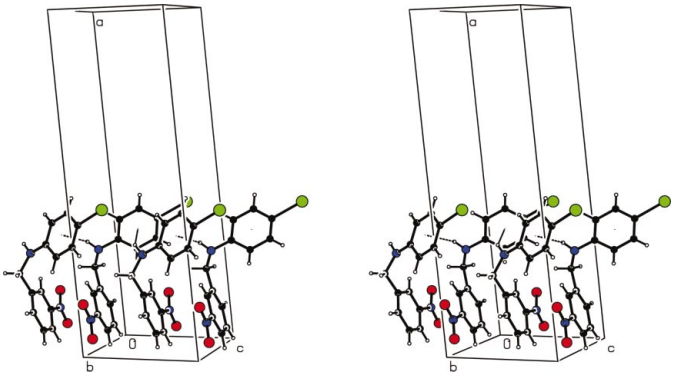

Figure 10
Stereoview of part of the crystal structure of (6) showing the formation of a chain along [001] by means of N—H···π(arene) hydrogen bonds and $\pi\cdots\pi$ stacking interactions.

Atom C33 in the nitrated ring of molecule 2 at (x, y, z) acts as a hydrogen-bond donor to O11 in molecule 1 at $(1 - x, -y, 1 - z)$: in combination with the N—H···O hydrogen bond within the asymmetric unit, this C—H···O hydrogen bond generates a centrosymmetric cyclic four-molecule aggregate, centred at $(\frac{1}{2}, 0, \frac{1}{2})$ and characterized by an $R_4^4(20)$ ring (Fig. 12). The formation of this aggregate is reinforced by one of the $\pi\cdots\pi$ interactions. The nitrated rings C31–C36 of the type 2 molecules at (x, y, z) and $(1 - x, -y, 1 - z)$ are parallel with an interplanar spacing of 3.385 (9) Å; the centroid separation is 3.685 (4) Å, corresponding to a near-ideal centroid offset of 1.46 (9) Å (Fig. 12).

These four-molecule aggregates are further linked by a combination of iodo···nitro and aromatic $\pi\cdots\pi$ stacking interactions to form the molecular ladder. Atom I42 in the type 2 molecule at (x, y, z) forms part of the cyclic aggregate centred at $(\frac{1}{2}, 0, \frac{1}{2})$: this I atom forms a weak two-centre iodo···nitro interaction with O32 in the type 2 molecule at $(-1 + x, 1 + y, z)$, which lies in the cyclic aggregate centred at $(-\frac{1}{2}, 1, \frac{1}{2})$. At the same time, the nitrated ring C11–C16 of molecule 1 at (x, y, z) forms a $\pi\cdots\pi$ stacking interaction with the iodinated ring C41–C46 of molecule 2 at $(-x, 1 - y, 1 - z)$, which is also a part of the cyclic aggregate centred at $(-\frac{1}{2}, 1, \frac{1}{2})$ (Fig. 13). In this manner the molecules are linked by the cooperative combination of four types of inter-

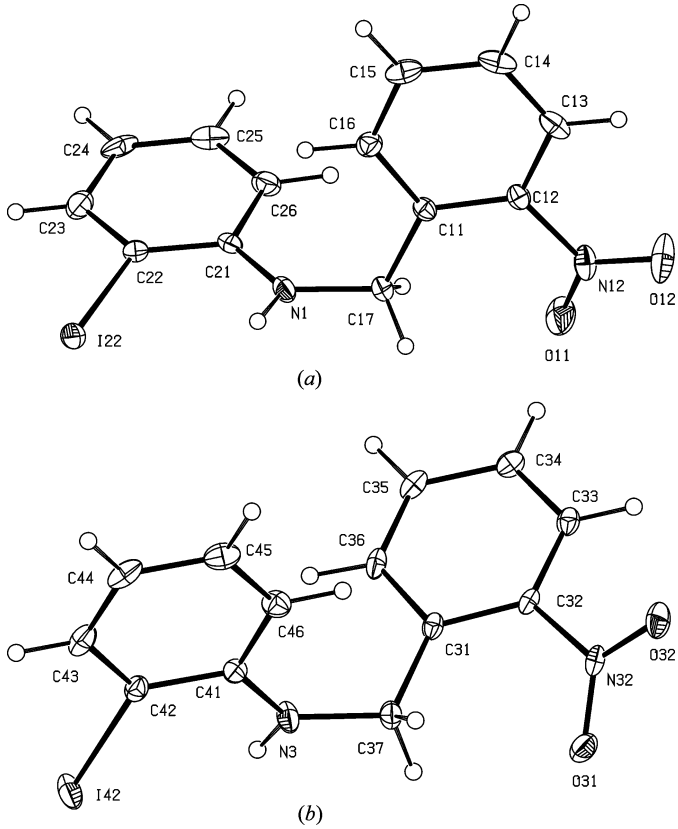

Figure 11
The two independent molecules of (7), showing the atom-labelling scheme: (*a*) molecule 1 and (*b*) molecule 2. Displacement ellipsoids are drawn at the 30% probability level.

molecular interactions into ladders running parallel to the [$\bar{1}$10] direction.

3.3. General comments on the supramolecular structures

The molecular constitutions of (1)–(9) [see (II)] allow the possibility of six different types of direction-specific intermolecular interaction. These are N—H···O and C—H···O, hydrogen bonds, iodo···nitro interactions, and aromatic $\pi\cdots\pi$ stacking interactions. In the event, no single compound in this series whose structure has been determined to date exhibits more than four of these types, while (1) exhibits only one type, namely C—H···O hydrogen bonds. Compounds (4)–(6) all exhibit three types of direction-specific intermolecular interaction, but the selection is, in fact, different for each: while the structures of all three of these compounds contain C—H···O hydrogen bonds, only that of (5) contains N—H···O and C—H···π(arene) hydrogen bonds, only that of (6) contains N—H···π(arene) hydrogen bonds, and only that of (4) contains iodo···nitro interactions. In addition, while the structures of both (4) and (6) contain aromatic $\pi\cdots\pi$ stacking interactions, these are absent from the structure of (5).

Not only do the number and identity of the types of intermolecular interactions vary, but the structural consequences of these interactions also show a wide range of behaviour. Thus, while (2) and (7) both contain the same four types of intermolecular interactions, namely N—H···O and C—H···O hydrogen bonds, and iodo···nitro and $\pi\cdots\pi$ stacking interactions, the consequences of these are entirely different in that the overall supramolecular structures of (2) and (7) are three- and one-dimensional, respectively. Compounds (1) and (7), exhibiting one and four types, respectively, in the intermolecular interactions, both have one-dimensional supramolecular structures; (5) and (6) both have two-dimensional supramolecular structures; (2) and (4), exhibiting four and three types, respectively, of intermolecular interaction, both have three-dimensional supramolecular structures.

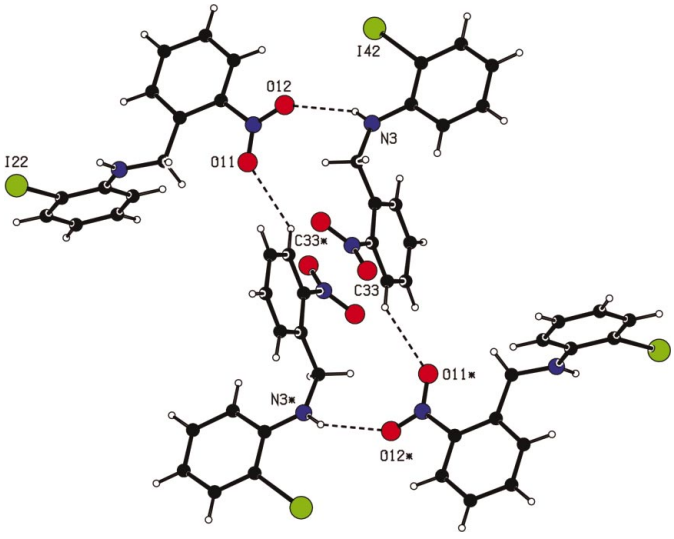

Figure 12
Part of the crystal structure of (7) showing the formation of a four-molecule aggregate containing an $R_4^4(20)$ ring. For the sake of clarity the unit-cell box has been omitted. The atoms marked with an asterisk (*) are at the symmetry position $(1-x, -y, 1-z)$.

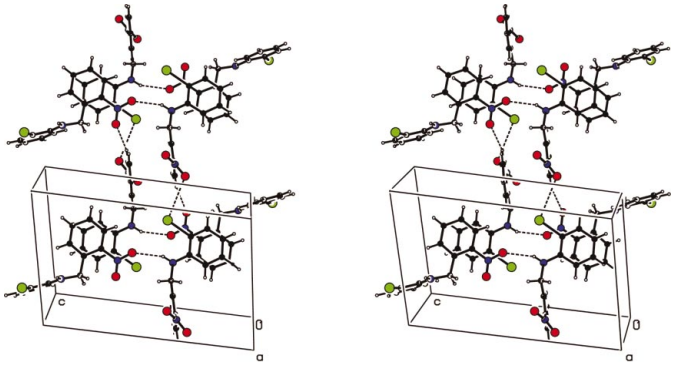

Figure 13
Stereoview of part of the crystal structure of (7) showing the iodo···nitro and $\pi\cdots\pi$ stacking interactions which link the $R_4^4(20)$ aggregates into a ladder along [$\bar{1}$10]. For the sake of clarity, H atoms bonded to C atoms are omitted.

4. Concluding comments

The molecular conformations of the isomeric iodo-*N*-(nitrobenzyl)anilines (see §3.1) and the patterns in their supramolecular aggregation (see §3.3) point to a subtle interplay of the weak direction-specific intermolecular forces. Weak forces of the types manifest here, dependent upon molecular polarizability and polarization, are not easy to model computationally. The variations in the supramolecular aggregation behaviour within an extended series of isomeric compounds, such as those described here, provide a keen test of computational methods for crystal-structure prediction (Lommerse *et al.*, 2000; Motherwell *et al.*, 2002): the accurate prediction of behaviour across such a series of isomeric species would generate real confidence in the efficacy of the predictive methods employed.

X-ray data were collected at the EPSRC X-ray Crystallographic Service, University of Southampton, England: the authors thank the staff of the Service for all their help and advice. JNL thanks NCR Self-Service, Dundee, for grants which have provided computing facilities for this work. JLW and SMSVW thank CNPq and FAPERJ for financial support.

References

Ferguson, G. (1999). *PRPKAPPA*. University of Guelph, Canada.
Flack, H. D. (1983). *Acta Cryst.* A**39**, 876–881.
Glidewell, C., Howie, R. A., Low, J. N., Skakle, J. M. S., Wardell, S. M. S. V. & Wardell, J. L. (2002). *Acta Cryst.* B**58**, 864–876.
Glidewell, C., Low, J. N., Skakle, J. M. S., Wardell, S. M. S. V. & Wardell, J. L. (2002). *Acta Cryst.* C**58**, o487–o490.
Kelly, C. J., Skakle, J. M. S., Wardell, J. L., Wardell, S. M. S. V., Low, J. N. & Glidewell, C. (2002). *Acta Cryst.* B**58**, 94–108.

Lommerse, J. P. M., Motherwell, W. D. S., Ammon, H. L., Dunitz, J. D., Gavezzotti, A., Hofmann, D. W. M., Leusen, F. J. J., Mooij, W. T. M., Price, S. L., Schweizer, B., Schmidt, M. U., van Eijck, B. P., Verwer, P. & Williams, D. E. (2000). *Acta Cryst.* B**56**, 697–714.
McArdle, P. (2003). *OSCAIL for Windows*, Version 10. Crystallography Centre, Chemistry Department, NUI Galway, Ireland.
Motherwell, W. D. S., Ammon, H. L., Dunitz, J. D., Dzyabchenko, A., Erk, P., Gavezzotti, A., Hofmann, D. W. M., Leusen, F. J. J., Lommerse, J. P. M., Mooij, W. T. M., Price, S. L., Schweizer, B., Schmidt, M. U., van Eijck, B. P., Verwer, P. & Williams, D. E. (2002). *Acta Cryst.* B**58**, 647–761.
Nonius (1997). *Kappa-CCD Server Software.* Windows 3.11 Version. Nonius BV, Delft, The Netherlands.
Otwinowski, Z. & Minor, W. (1997). *Methods Enzymol.* **276**, 307–326.
Sheldrick, G. M. (1997*a*). *SHELXL*97. University of Göttingen, Germany.
Sheldrick, G. M. (1997*b*). *SHELXS*97. University of Göttingen, Germany.
Spek, A. L. (2003). *J. Appl. Cryst.* **36**, 7–13.
Starbuck, J., Norman, N. C. & Orpen, A. G. (1999). *New J. Chem.* **23**, 969–972.
Wardell, J. L., Wardell, S. M. S. V., Skakle, J. M. S., Low, J. N. & Glidewell, C. (2002). *Acta Cryst.* C**58**, o428–o430.
Wilson, A. J. C. (1976). *Acta Cryst.* A**32**, 994–996.